

Density of states of disordered topological superconductor-semiconductor hybrid nanowires

Jay D. Sau¹ and S. Das Sarma²

¹*Department of Physics, Harvard University, Cambridge, MA 02138*

²*Condensed Matter Theory Center and Joint Quantum Institute, Department of Physics, University of Maryland, College Park, Maryland 20742-4111, USA.*

Using Bogoliubov-de Gennes (BdG) equations we numerically calculate the disorder averaged density of states of disordered semiconductor nanowires driven into a putative topological p -wave superconducting phase by spin-orbit coupling, Zeeman spin splitting and s -wave superconducting proximity effect induced by a nearby superconductor. Comparing with the corresponding theoretical self-consistent Born approximation (SCBA) results treating disorder effects, we comment on the topological phase diagram of the system in the presence of increasing disorder. Although disorder strongly suppresses the zero-bias peak (ZBP) associated with the Majorana zero mode, we find some clear remnant of a ZBP even when the topological gap has essentially vanished in the SCBA theory because of disorder. We explicitly compare effects of disorder on the numerical density of states in the topological and trivial phases.

PACS numbers: 03.67.Lx, 03.65.Vf, 71.10.Pm

I. INTRODUCTION

The theoretical prediction¹⁻⁶ that the combination of spin-orbit coupling, Zeeman spin splitting, and ordinary s -wave superconductivity could lead to an effective topological superconducting phase under appropriate (and experimentally achievable) conditions has led to an explosion of theoretical and experimental activities⁶ in semiconductor nanowires (InSb or InAs) in proximity to a superconductor (NbTi or Al) in the presence of an external magnetic field. The experimental finding⁷ of a ZBP, in precise agreement with the theoretical predictions in the differential tunneling conductance of an InSb nanowire (in contact with a NbTiN superconducting substrate) at a finite external magnetic field ($B \sim 0.1 - 1$ T), followed by independent corroborative observation⁸⁻¹¹ of such ZBP both in InSb and InAs nanowires in contact with superconducting Nb and Al by several groups, has created excitement in the condensed matter physics community as well as the broader scientific community as perhaps the first direct evidence supporting the existence of the exotic, the elusive, and the emergent unpaired Majorana bound state in solids. Such excitement has invariably been followed by a wave of skepticism as one would expect in a healthy and active scientific discipline with questions ranging all the way from whether such ZBP could arise from other (i.e. non-Majorana) origin to whether all aspects of the observed experimental phenomenology are consistent with the putative theoretical predictions on the topological superconductivity underlying the existence of the Majorana mode.

One particular issue, which is also the subject of the current work, attracting a great deal of theoretical attention¹²⁻²⁴ is the role of disorder in the Majorana physics of superconductor-semiconductor hybrid structures. Disorder plays a key role in the Majorana physics because the underlying topological super-

conducting phase hosting the Majorana mode (at defect sites) is essentially an effective spinless p -wave superconductor¹⁻⁵, which, unlike its s -wave counterpart, is not immune to non-magnetic elastic disorder (i.e. spin-independent momentum scattering) as was already known ten years ago²⁵. Thus, even the simplest kind of disorder, namely zero-range random non-magnetic point elastic scatterers in the wire, could strongly affect the topological superconductivity in contrast to ordinary s -wave superconductivity which is immune to non-magnetic disorder, and the associated Majorana bound states by suppressing the (topological) superconducting gap¹³ and/or creating Andreev bound states in the superconducting gap near zero-energy¹⁴ complicating the observation and the interpretation of the ZBP. We do, however, mention that elastic disorder or momentum scattering in the superconductor itself, no matter how strong (as long as it does not destroy the superconductor), does not affect the topological superconducting phase in the semiconductor.²¹ In addition, it has recently been emphasized that elastic disorder by itself could create a zero-bias peak (essentially, an anti-localization peak associated with the disorder-induced quantum interference) in the non-topological phase in the presence of spin-orbit coupling and Zeeman splitting. Since the precise topological quantum critical point (as a function of the applied magnetic field) separating the topological and the trivial superconducting phase is in general not known in the experiments,⁷⁻¹² one cannot be absolutely sure that the observed ZBP is indeed a Majorana bound state (MBS) signature in the topological phase and not a trivial anti-localization peak in the non-topological phase.

In the current work we consider disorder effects on MBS physics by directly calculating the density of states (DOS) of finite disordered nanowires in the presence of proximity-induced superconductivity taking into account spin-orbit coupling and spin splitting arising respectively from Rashba and Zeeman effects in the wire.

We use random uncorrelated point scatterers with δ -function potential in the wire to represent the elastic disorder. The theory follows the standard prescription²⁶ of an exact diagonalization of the BdG equations in a minimal tight-binding model including superconducting pairing, Rashba spin-orbit coupling, and Zeeman splitting in the Hamiltonian. The diagonalization of the discretized tight-binding Hamiltonian leads to the exact eigenstates of the system, which then immediately give the density of states (theoretical details are available in Ref. 26 and are not repeated here.) Comparison with theory in the presence of disorder necessitates the ensemble averaging over many different impurity configurations since each disorder configuration produces its own unique result with random impurity-induced delta-function peaks in the superconducting gap.

II. DOS IN THE DISORDERED TOPOLOGICAL PHASE

In this section, we consider the effect of disorder on the SM/SC system starting from the topological phase in the clean limit. In Fig. 1 (with 8 panels, each representing a different strength of disorder keeping all other parameters fixed), we show our numerical DOS as a function of energy (E) for different relevant parameter sets in the topological phase of the system. We show both the ensemble averaged DOS using many-impurity configurations (but using the same disorder strength, i.e. the same impurity density and potential strength, changing only the random localities of the impurities along the wire) and the typical DOS for a single impurity configuration in each case. Each panel corresponds to a specific disorder strength (i.e. a fixed impurity density) and shows results for three different lengths of the nanowire.

Since our calculations follow either Ref. 26 for the exact numerical treatment of Ref. 13 for the SCBA theory, we refer the reader to those references for the technical details, which are actually pretty standard.^{19–22}

The superconductor (SC)-semiconductor (SM) hybrid nanowire structure is characterized by a large number of independent parameters, both for the actual experimental laboratory systems and for our minimal theoretical model. The minimal set of parameters necessary to describe the system are the proximity-induced SC gap (Δ_0) in the SM, the parent SC pairing potential (Δ_s), the Rashba spin-orbit coupling (α_R), the spin splitting (V_Z), the chemical potential (μ), the SM effective mass (m) which defines the SM tight-binding hopping parameter, the nanowire length (L), and disorder (which we take to be the uncorrelated random white noise potential associated with randomly located δ -function in real space spin-independent scattering centers). There are a few additional physically important parameters which are, however, not independent parameters of the theory: the coherence length in the nanowire (ξ), the SM mean-free path (λ) due to disorder, and the number of

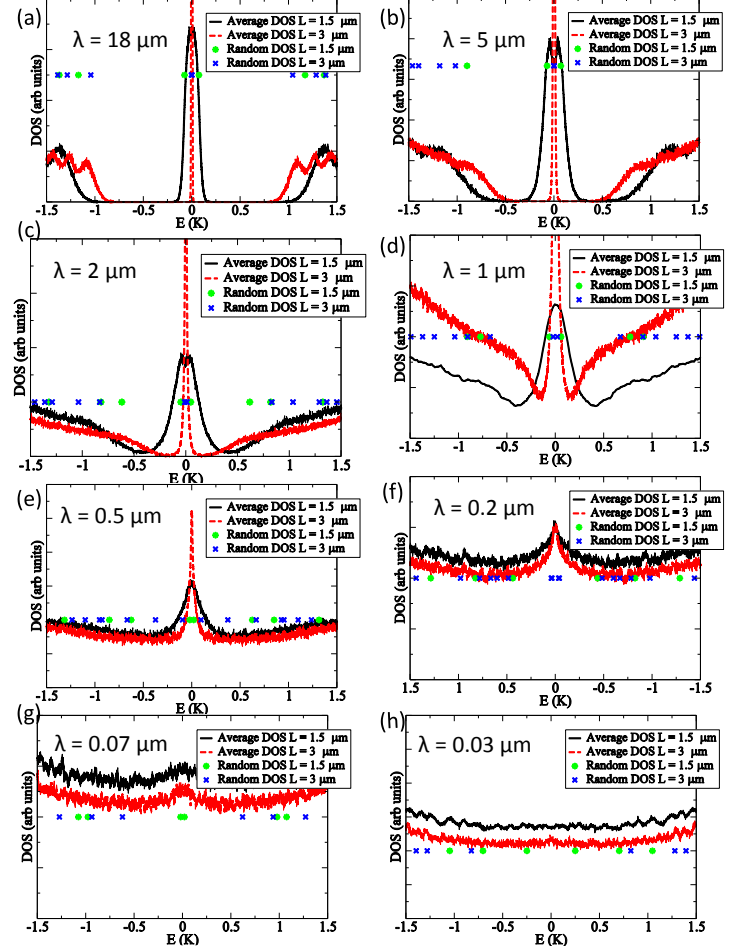


FIG. 1. Disorder averaged density of states in the topological phase for the semiconductor nanowire in a magnetic field with Zeeman splitting $V_Z = 5$ K, proximity-induced pairing potential of amplitude $\Delta_0 = 3$ K, Rashba spin-orbit coupling strength $\alpha_R = 0.3$ eV-Å. For this choice of parameters the clean quasiparticle-gap $\Delta = 1.3$ K and coherence length $\xi = 0.3$ μm . The difference panels (a-h) correspond to different disorder strengths characterized by $E_s = \hbar/2\tau = 10, 50, 100, 200, 460, 1300, 3300, 7300$ mK. The corresponding mean-free paths are λ are in the panels and the self-consistent Born gaps $E_{SCB} = 1.2, 1.1, 0.9, 0.8, 0.13, 0, 0, 0$ K.

occupied subbands (i.e. transverse quantized levels) in the nanowire which we take to be one throughout assuming the system to be in the one-dimensional limit. (The single sub-band approximation, made entirely for the convenience of keeping the number of parameters in the model to be tractable, is a nonessential approximation, and our qualitative results should be completely independent of this approximation.) In addition, there is an independent parameter defining the hopping amplitude across the SC/SM interface which controls the proximity-induced SC pairing gap Δ_0 in the SM in terms of the parent gap Δ_s in the SC. Finally, the proximity gap (Δ) in the SM in the presence of spin-orbit cou-

pling and finite Zeeman splitting is reduced from Δ_0 in a known manner. All the details for modeling the disorder are given in Ref. 13 where SCBA was used in contrast to our exact numerical diagonalization in the current work following Ref. 26. One specific goal of our current work is to compare the analytic and simple SCBA theory¹³ with the exact tight-binding numerical analysis to test the limits of validity and the applicability of the SCBA theory which, being analytic, can be used rather easily.

We choose parameters approximately consistent with the InSb/Nb systems studied experimentally in⁷. These are : $\Delta_0 = 3\text{K}$, $\alpha_R = 0.3\text{eV} - \text{\AA}$ (corresponding to an effective spin-orbit coupling strength $m^*\alpha_R^2 = 2.5\text{K}$). Since our interest is in disorder effects, we focus on a range of magnetic fields with a spin splitting $V_Z \sim 5\text{K}$ (we vary it in a few cases only to change the proximity to the topological quantum phase transition point, separating the topological and the trivial SC phase). Given that the condition for the topological SC phase to be realized in the SM is given by² $V_Z > \Delta^2 + \mu^2$, where Δ is the actual induced gap in the SM, the system should be in the MBS carrying topological phase for $\Delta < 5\text{K}$ (since $\mu = 0$). Given that $\Delta < \Delta_0 = 3\text{K}$, with the reduction of Δ below Δ_0 arising from the existence of $V_Z \neq 0$, our system is deep in the topological phase for the results shown in Fig.1 since $V_Z (= 5\text{K}) \gg \Delta (= 1.3\text{K})$ and $\mu = 0$.

Each panel in Fig. 1 corresponds to a different disorder strength in the system, characterized by the corresponding level broadening $E_s = \hbar/2\tau$ (where τ is the scattering time – $\tau = \infty$ in the absence of disorder) or equivalently the mean free path $\lambda = v_F\tau$ (where v_F is the fermi velocity), both calculated in the SCBA according to Ref. 13 for the given disorder in the wire. In each panel (and for each disorder) we show our DOS numerical results for two distinct wire lengths $L = 1.5\mu\text{m}$ and $L = 3\mu\text{m}$. In each case, we show both the ensemble averaged DOS results using an averaging over many (> 1000) random impurity configurations (keeping E_s, λ etc fixed) and the result for a typical single impurity configuration (the distinct crosses or dots denoting delta functions for the DOS at the value of energy). We emphasize that for an infinitely long wire ($L \gg \xi \approx 0.5\mu\text{m}$ for our case) the DOS in the absence of disorder will vanish throughout the gap ($\pm 1.3\text{K}$ in our case) with a δ -function peak at $E = 0$ associated with the MBS at the wire edges.

To characterize the disorder strength for the results in Fig. 1 (with panels (a) to (h) with increasing disorder keeping all other parameters fixed), we use SCBA for this problem which was developed by us in Ref. 13. The SCBA theory provides us with the SC gap in the topological phase for a given disorder strength, allowing us to compare our direct (and exact) numerical calculation in the presence of disorder with the SCBA theory. We show the calculated SCBA gap in each case in the figure captions for the sake of direct comparison with the exact results in the figures. (The SCBA theory is obviously an ensemble averaged theory for the infinite system and does not depend on L .) It is clear from the result of Fig.

1 that the analytical SCBA theory of Ref. 13 are in excellent qualitative agreement with the exact ensemble-averaged numerical results for the DOS even for $E_s \approx \Delta$, where the topological gap essentially vanishes (panel (e) in Fig. 1) both according to the SCBA (i.e. $E_{SCB} = 0$) and in our numerical results. While the disorder averaged DOS calculated by exact diagonalization does not strictly vanish inside the gap, the gap calculated with the SCBA can be identified with the peaks in the DOS at the edges of the gap. The closing of the gap within the SCBA coincides with the disappearance of the dips in the DOS around zero-energy. The DOS peak at $E = 0$ associated with the MBS is continuously suppressed with increasing disorder, but quite amazingly there is a discernible DOS peak at $E = 0$ even for $E_s (= 3.3\text{K}) \gg \Delta (= 1.3\text{K})$ where $E_{SCB} = 0$, and at best the topological superconductivity is gapless.

The remarkable result, which is quite apparent in our Figs. 1 (e)-(g), is that the MBS peak of the DOS at $E = 0$ is actually very robust to disorder and survives disorder strength substantially larger than that (typically $E_s \sim \Delta$) destroying the induced superconducting gap Δ . Thus, in Figs. 1(e)-(g), although the SCBA theory and our exact numerical results both show the system to be gapless with $E_s > \Delta$, the DOS peak at $E = 0$ associated with the MBS persists until $E_s \gg \Delta$ as in Fig. 1(h) where $E_s = 7\text{K} (\gg \Delta = 1.3\text{K})$. It is not only that the MBS feature in the ensemble averaged DOS survives up to very strong disorder (e.g. the mean free path $\lambda = 0.5\mu\text{m}, 0.2\mu\text{m}$ and $0.06\mu\text{m}$ respectively in Figs. 1(e)-(g) which are smaller than the wire lengths of $L = 1.5\mu\text{m}$ and $3\mu\text{m}$ used in our numerical work), the typical DOS for single random impurity configuration also shows peaks at $E = 0$ as can clearly be seen in Figs. 1(e)-(g) [and as well as in Figs. 1(a)-(d)], but not in Fig. 1(h) where the very large disorder strength ($\lambda = 0.02\mu\text{m}$) suppresses both the ensemble averaged MBS peak as well as the single configuration peak at $E = 0$. The survival of the zero-energy DOS peak well above the point where the SC gap is completely suppressed by disorder is an important new result of our exact numerical work directly establishing the possible theoretical existence of a gapless topological SC phase.

A. Griffiths effects

The origin of the $E = 0$ peak in the DOS in the strongly disordered case can be related to the Griffiths effect previously considered for the spinless p -wave superconductor²⁵. The Griffiths effect in the semiconductor nanowire at finite V_Z arises from the disorder-induced variation of the chemical potential, which can lead to a transition from a topological phase to a non-topological phase and vice-versa. The variation of the effective chemical potential can lead to domain-walls between topological and non-topological regions each of which would support a local zero-energy MBS. Since each region is of

finite extent, the MBSs are a finite distance apart and split into conventional states with a non-zero energy. In fact, by carefully considering the distribution of the distances between the MBSs, it has been shown²⁵ that this splitting typically leads to a singular peak in the DOS at $E = 0$, which diverges as $E \rightarrow 0$ as a power-law in E . The topological phase is of course characterized by true zero-energy edge states, whose energy is exponentially small in the length of the system L . Thus, in the long wire limit, the topological phase and the non-topological phase both have power-law divergent DOS due to the Griffiths effects, but the topological phase has a pair of zero-modes exponentially close to zero energy¹². This distinction between exponential versus power-law in the length seems to appear in the DOS plotted in Fig 1. At small disorder, there is a sharp peak which is very weakly split. At larger disorder (panels (e,f,g,h)), which is approximately when the gap vanishes i.e. $E_{SCBA} \rightarrow 0$, the $E \sim 0$ peak in the DOS is broadened.

For finite length systems, the sharp transition between the topological and non-topological phase at finite disorder becomes a crossover. While the topological invariant can be computed even for a disordered, but strictly infinite system^{12,23,24}, we have not done so in the present work because we restrict ourselves to systems of wire lengths comparable to the experimental systems. For such finite wires the distinction between the topological and non-topological phase is not sharp. In fact, the zero-modes arising from the Griffiths effect are themselves MBSs. The MBSs characterizing the topological phase are special only in the sense that they occur near the ends of a finite system and are therefore separated from other low-energy MBSs by a distance of the order of the length of the wire. This can also occur from the Griffiths effect in some realizations of disorder, even in the non-topological parameter regime. Therefore, the Griffiths singularities seen in the disordered Fig. 1 indicate the presence of several low-lying MBSs in the spectrum of the finite wire. For very large disorder the system becomes completely non-topological (and gapless) as in Fig. 1(h).

There are three important messages following from our DOS results for the topological phase in the presence of disorder: (1) the zero-energy DOS peak associated with the MBS is strongly suppressed by disorder; (2) SCBA is an excellent quantitative approximation for calculating the SC gap in the topological phase including effects of disorder; and (3) most importantly, the zero-energy MBS peak is very robust against disorder and survives well after the SC gap in the topological phase has been suppressed to zero, and disappears only when the mean free path $\lambda \lesssim \xi/6$ or $E_s \gtrsim 6\Delta$ (for the systems are studied) whereas the topological SC gap vanishes for $\lambda \lesssim \xi$.

Given the quantitative validity of the SCBA, we can calculate the phase diagram of the SC/SM structure in the presence of disorder by using the analytical SCBA theory.¹³ We show our SCBA-calculated quantum phase diagram of the system in Fig. 2. In Fig. 2, we fix all pa-

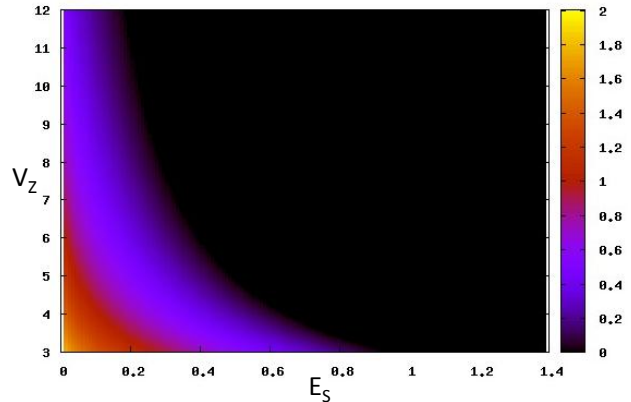


FIG. 2. Quasiparticle gap Δ (in the color bar) versus Zeeman potential V_Z and scattering rate E_s in the topological phase. The black region represents the gapless phase and is therefore not topologically robust.

rameters except for disorder (E_s) and spin-splitting (V_Z) with the color representing the calculated SC gap E_{SCBA} in the presence of disorder (by definition $E_{SCBA} = \Delta$ for $E_s = 0$). The black region represents gapless superconductivity. We note, based on our numerical results of Fig. 1, that a large part of the black region in the phase diagram allows for well-defined zero-energy DOS MBS peaks although the system is essentially a gapless topological superconductor in this regime. Much of this SCBA gapless regime is dominated by Griffiths physics except for very large disorder when the system eventually becomes nontopological (i.e. even the finite topological segments disappear). Much of this SCBA gapless regime is dominated by Griffiths physics except for very large disorder when the system eventually becomes non-topological. Except for our current results showing the well-defined robust persistence of the MBS peak even in the gapless topological regime (the black region in Fig. 2), one would have concluded that SCBA predicts a rather gloomy picture for the existence of the Majorana mode in the disordered SC/SM hybrid structure since, without our current exact results, the conclusion would have been that there cannot be any MBS in the black region of the phase diagram. Of course the quantitative details of the SCBA phase diagram depend on the SO-coupling strength and the topological phase with a large SC gap is easily achieved by large (small) SO coupling (disorder).

III. DOS IN THE DISORDERED NON-TOPOLOGICAL PHASE

Next we comment on the effect of disorder in the non-topological SC regime, i.e., for $V_Z < \sqrt{\Delta^2 + \mu^2}$ for the

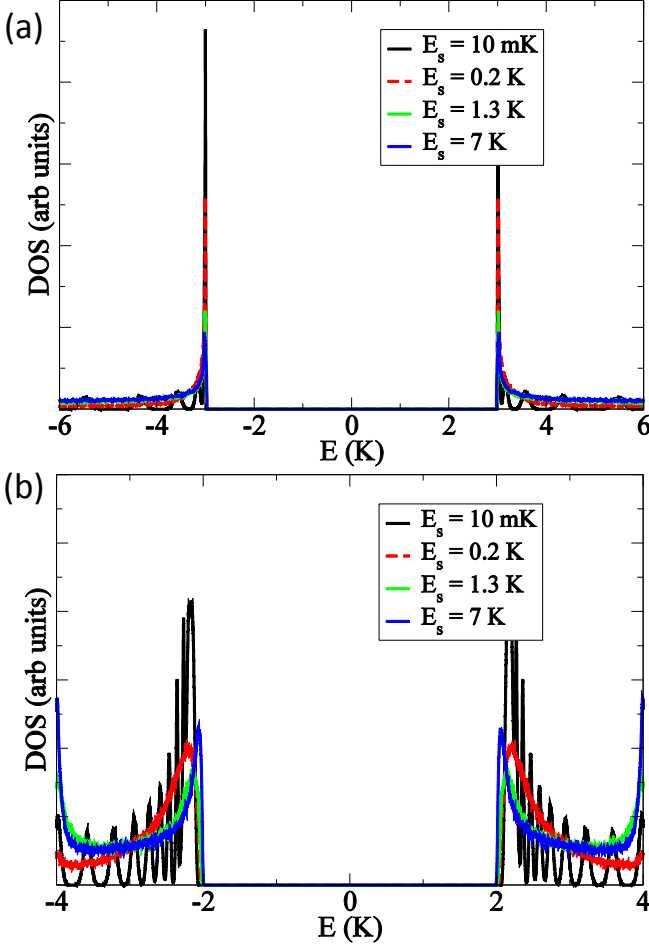


FIG. 3. Disorder averaged density of states in the non-topological phase for the semiconductor nanowire in a magnetic field with Zeeman splitting $V_Z = 0, 1 K$ (panels (a, b) respectively) at $\mu = 0$ for different disorder strengths characterized by scattering rates $E_s = \hbar/\tau$.

SC/SM hybrid structure. In Fig. 3(a) and (b), we show our calculated numerical DOS in the non-topological SC phase (for $\mu = 0$) for $V_Z = 0$ (3a) and $1 K$ (3b) in the presence of disorder. All parameters other than V_Z are exactly the same as in Fig. 1. We see that, at least for $\mu = 0$, the behavior of the DOS is similar to a classic s -wave SC (even for $V_Z = 1 K$ which simply reduces the gap from $\Delta_0 = 3 K$ to $2 K$) with essentially no discernible effect on the DOS. Even for disorder as large as $E_s > 7 K > 2\Delta_0$, we do not see any structure developing in the SC DOS gap which remains completely flat. For $V_Z = 0$ (Fig. (3a)) this is a direct consequence of Anderson's theorem where the robustness of the gap arises from time-reversal symmetry. We see in Fig. (3b) that this behavior persists for small Zeeman fields as long as $V_Z \lesssim \Delta$. This behavior can be expected based on previous studies on the bound states of single impurities in spin-orbit coupled nanowires in proximity to superconductors²⁷. There

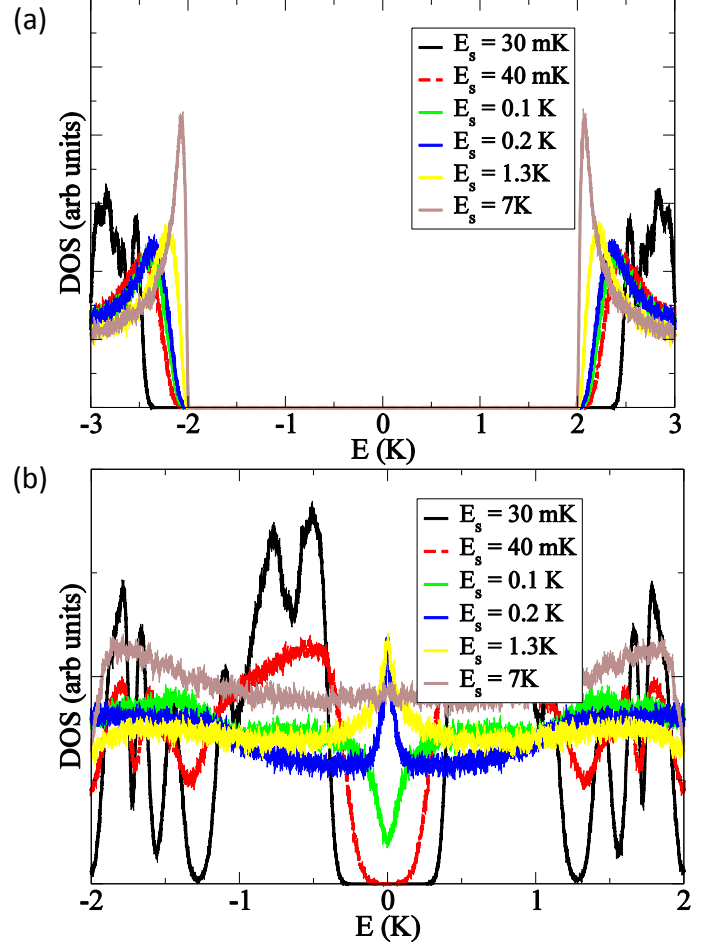


FIG. 4. Disorder averaged density of states in the non-topological phase for the semiconductor nanowire in a magnetic field with Zeeman splitting $V_Z = 4, 5 K$ (panels (a, b) respectively) at $\mu = 5 K$ for different disorder strengths characterized by scattering rates $E_s = \hbar/\tau$.

it was found that the low-energy sub-gap states appear for short-ranged impurities only in the topological phase. However, this conclusion might not apply to longer-range disorder because in principle, at any non-zero value of Zeeman potential puddles can lead to the formation of a pair of low-energy MBSs. In our numerical work here we restrict ourselves only to zero-range white noise disorder in the semiconductor.

The situation, however, changes qualitatively when we consider the limit $V_Z \gtrsim \Delta$. We show these results in Fig. 4 where $V_Z = 1 K$, $\mu = 5 K$ and $V_Z = \mu = 5 K$ are shown for several values of the disorder parameter $E_s (\equiv \hbar/2\tau)$. All other parameters are the same as in Fig. 1 and 2. We note that the situation in Fig. 4 describes the non-topological phase since $V_Z = \mu < \sqrt{\mu^2 + \Delta^2}$. In both panels, large disorder has a strong effect on the SC DOS shrinking the SC gap considerably. However, in Fig. 4(b), where $V_Z \gg \Delta$, eventually for $E_s = 0.2 K$

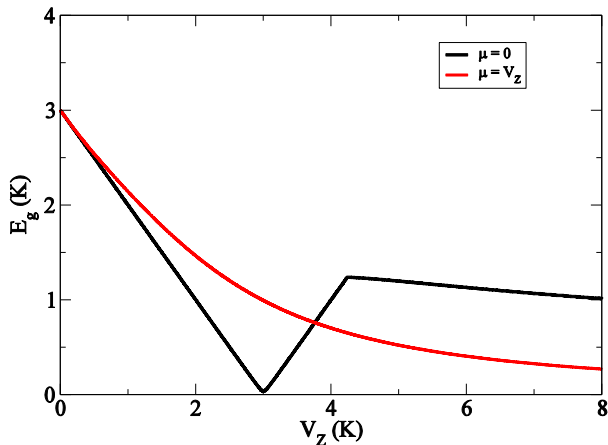


FIG. 5. Quasiparticle gap (Δ) versus Zeeman potential V_Z for different values ($\mu = 0, 5K$) for the chemical potential μ . The vanishing of the quasiparticle gap marks the topological quantum phase transition from the non-topological phase at small V_Z to the topological phase at large V_Z .

and $1.3 K$ (and $V_Z = \mu = 5 K$), the DOS seems to "flip" and the dip at $E = 0$ becomes a peak at $E = 0$ with a concomitant vanishing of any SC gap feature in the data. For even larger E_s ($E_s = 7 K$ in Fig. 4) the peak feature in the DOS is suppressed, but there is a clear $E = 0$ DOS peak for intermediate (but still large with $E_s > \Delta$) disorder ($E_s = 0.2 K$ and $1.3 K$ in Fig. 4) where the SC gap has disappeared, but a peak has developed in the DOS at zero-energy. We believe that the zero-energy DOS peak in Fig. 4(b) for $E_s = 0.2 K$ and $1.3 K$ has the same origin as the physics recently discussed in several publications^{16–18}. The hallmark of this "trivial" DOS peak (arising from the competition among spin splitting, spin-orbit coupling, and superconductivity) are that (1) it arises only for large Zeeman splitting in the non-topological phase; (2) it occurs only after the SC quasiparticle gap has been completely suppressed by disorder; (3) it exists only in an intermediate disorder range where the superconducting quasiparticle gap has been suppressed, vanishing for larger disorder and the peak becoming a dip (i.e. the SC gap) for smaller disorder.

In order to specify where precisely in the phase diagram we are obtaining our exact numerical results in the presence of disorder we finally show in Fig. 5 our calculated SC gap as a function of V_Z (for zero disorder) for the parameters chosen in our calculations. For $\mu = 0$ (i.e. Figs. 1-3), the topological quantum phase transition (TQPT) happens at $V_Z = \Delta_0 (= 3 K$ in our choice), and our Fig. 1 belongs to the topological phase ($V_Z = 5 K$, to the right of the TQPT) whereas our Fig. 2 belongs to the non-topological ($V_Z = 0, 1 K$) to the left of the TQPT. Results for Fig. 4 are obtained for $V_Z = \mu$ (and $V_Z < \mu$) which never can manifest a TQPT since the

$V_Z = \sqrt{\mu^2 + \Delta^2}$ condition cannot be satisfied except for $\Delta = 0$ (i.e. $V_Z \rightarrow \infty$)— but, even the nontopological SC is strongly affected by disorder (for $V_Z \gg \Delta$) here since the combination of spin-orbit coupling and Zeeman splitting makes the Anderson theorem moot. Thus the DOS peak in Fig. 4, associated with anti-localization,^{16–19} arises purely in the trivial phase with a completely suppressed quasiparticle gap which might enable its experimental distinction from the MBS peak in the topological SC phase.

IV. DISCUSSION

Finally we mention that the spin-orbit coupled semiconductor system thus has two distinct topological quantum phase transitions in the presence of the superconducting proximity effect and Zeeman splitting. The first one is driven by the Zeeman field as originally predicted by Sau et al² with the TQPT defined by $V_Z = \sqrt{\mu^2 + \Delta^2}$ assuming a low disorder situation. The second one is driven by increasing disorder (E_s) in the finite Zeeman splitting situation (i.e. $V_Z > \sqrt{\mu^2 + \Delta^2}$) where the topological SC phase is destroyed by disorder (for $E_s \gtrsim \Delta$), leading to a gapless non-topological phase dominated by the Griffiths physics as originally envisioned by Motrunich et al²⁵. Since the effective SC gap for $V_Z \neq 0$ depends on V_Z , and in particular, $\Delta \propto V_Z^{-1}$ for $V_Z \gg \Delta_0$ [see Refs. 5 and 13 for details], we expect that there are two distinct magnetic field driven TQPTs in the semiconductor nanowires - - the first one is the TQPT predicted in Ref. 2–5 taking the system from the trivial s -wave SC (induced by proximity effect) to the (effective p -wave) topological Majorana carrying p -wave SC phase at low disorder (i.e. $\Delta \gg E_s$), and then the second one at much higher Zeeman splitting (so that $\Delta \lesssim E_s$) where disorder drives the system from a gapless topological SC to a non-topological Griffiths phase. It is unlikely that this second (purely disorder driven) TQPT would be experimentally accessible since the gapless nature of the SC phase (i.e. black region in Fig. 2 or the situation corresponding to Fig. 1 (e)-(h)) would make the finite temperature of the experimental system behave like a very high temperature (i.e. $T \gg \Delta$), making any experimental study of this disorder-driven TQPT difficult, if not impossible. Thus, the effective gapless nature of the system in Fig. 1(e)-(g) would make it very unlikely that the DOS peak (which is quite obvious in our theoretical results) could be studied experimentally. The best hope for the direct experimental study of the MBS physics is therefore to have a large SC gap (as in Fig. 1(a)-(d) or in the non-black region of Fig. 2) in the topological phase which necessitates having low effective disorder ($E_s \ll \Delta$), a condition guaranteed by having very clean semiconductor wires and/or very strong SO coupling in the material. We add here that our theoretical results presented in this paper cannot be compared (or connected) with the experiments in any way since we only calculate bulk DOS

of the system, which cannot be directly probed experimentally.

V. CONCLUSION

In summary, we have studied the disorder averaged DOS of a disordered spin-orbit coupled nanowire in proximity to a superconductor in both the topological and non-topological parameter regime. The features in the DOS associated with the superconducting gap in the topological phase appear to be in good quantitative agreement with the SCBA from previous work¹³. Consistent with previous results¹³, we find that the dips in the DOS associated with the quasiparticle gap disappear for

relatively modest ($E_s \gtrsim \Delta$) amounts of disorder. However, a zero-energy peak associated with MBSs generated by the Griffiths effect survives to much higher levels of disorder. The DOS peak associated with different levels of disorder arising from the Griffiths effect starting from the topological phase and the antilocalization peak starting from the non-topological phase appear to be different enough that one might distinguish them qualitatively. Of course, at this point one does not expect a sharp distinction between the peak arising from the Griffith's effect and the antilocalization effect because they are zero energy peaks in the DOS in the non-topological phase in the same symmetry class i.e. class D.

This work is supported by Microsoft Q, JQI-NSF-PFC, and the Harvard Quantum Optics Center.

-
- ¹ C. W. Zhang, S. Tewari, R. M. Lutchyn, S. Das Sarma, Phys. Rev. Lett. **101**, 160401 (2008); M. Sato, Y. Takahashi, S. Fujimoto, Phys. Rev. Lett. **103**, 020401 (2009).
 - ² Jay D. Sau, R. M. Lutchyn, S. Tewari, S. Das Sarma, Phys. Rev. Lett. **104**, 040502 (2010).
 - ³ R. M. Lutchyn, Jay D. Sau, S. Das Sarma, Phys. Rev. Lett. **105**, 077001 (2010).
 - ⁴ Y. Oreg, G. Refael, F. V. Oppen, Phys. Rev. Lett. **105**, 177002 (2010).
 - ⁵ J. D. Sau, S. Tewari, R. Lutchyn, T. Stanescu and S. Das Sarma, Phys. Rev. B **82**, 214509 (2010).
 - ⁶ See, e.g. T. Stanescu and S. Tewari, arXiv:1302.5433 (2013) for a review; C. W. J. Beenakker, arXiv:1112.1950 (2011); J. Alicea, Rep. Prog. Phys. **75**, 076501 (2012); M. Leijnse and K. Flensberg Semicond. Sci. Technol. **27**, 124003 (2012).
 - ⁷ V. Mourik, K. Zuo, S. M. Frolov, S. R. Plissard, E. P. A. M. Bakkers and L. P. Kouwenhoven, Science **336**, 1003 (2012).
 - ⁸ M. T. Deng, C. L. Yu, G. Y. Huang, M. Larsson, P. Caroff, H. Q. Xu, Nano Lett. **12**, 6414 (2012).
 - ⁹ A. Das, Y. Ronen, Y. Most, Y. Oreg, M. Heiblum, H. Shtrikman, Nat. Phys. **8**, 887 (2012).
 - ¹⁰ A. D. K. Finck, D. J. Van Harlingen, P. K. Mohseni, K. Jung, X. Li, Phys. Rev. Lett. **110**, 126406 (2013).
 - ¹¹ H. O. H. Churchill, V. Fatemi, K. Grove-Rasmussen, M. T. Deng, P. Caroff, H. Q. Xu, C. M. Marcus, arXiv:1303.2407 (2013).
 - ¹² P. W. Brouwer, M. Duckheim, A. Romito, and F. von Oppen, Phys. Rev. Lett. **107**, 196804 (2011); P. W. Brouwer, M. Duckheim, A. Romito, F. von Oppen, Phys. Rev. B **84**, 144526 (2011).
 - ¹³ J. D. Sau, S. Tewari, S. Das Sarma Phys. Rev. B **85**, 064512 (2012).
 - ¹⁴ A. M. Lobos, R. M. Lutchyn, S. Das Sarma, Phys. Rev. Lett. **109**, 146403 (2012).
 - ¹⁵ T. D. Stanescu, R. M. Lutchyn, S. Das Sarma, Phys. Rev. B **84**, 144522 (2011).
 - ¹⁶ J. Liu, A. C. Potter, K.T. Law, P. A. Lee, Phys. Rev. Lett. **109**, 267002 (2012).
 - ¹⁷ D. Bagrets and A. Altland Phys. Rev. Lett. **109**, 227005 (2012).
 - ¹⁸ P. Neven, D. Bagrets, A. Altland arXiv:1302.0747 (2013).
 - ¹⁹ D. I. Pikulin, J. P. Dahlhaus, M. Wimmer, H. Schomerus, C. W. J. Beenakker, New J. Phys. **14**, 125011 (2012).
 - ²⁰ S. Takei, B. M. Fregoso, H-Y Hui, A. M. Lobos, S. Das Sarma, arXiv:1211.1029 (2012).
 - ²¹ R. M. Lutchyn, T. D. Stanescu, S. Das Sarma, Phys. Rev. B **85**, 140513(R) (2012).
 - ²² E. Prada, P. San-Jose, R. Aguado, Phys. Rev. B **86**, 180503(R) (2012) ; C. Bena et al arXiv:1301.7420
 - ²³ I. C. Fulga, F. Hassler, A. R. Akhmerov, C. W. J. Beenakker Phys. Rev. B **83** 155429 (2011).
 - ²⁴ I. Adagideli, M. Wimmer, A. Teker, arXiv:1302.2612 (2013).
 - ²⁵ O. Motrunich, K. Damle, D. Huse, Phys. Rev. B **63**, 224204 (2001).
 - ²⁶ C-H Lin, J. Sau, S. Das Sarma, Phys. Rev. B **86**, 224511 (2012).
 - ²⁷ J. Sau, E. Demler, arXiv:1204.2537(2012).